

Study of Electron Spin Resonance on single crystals $EuFe_{2-x}Co_xAs_2$

J. J. Ying, T. Wu, Q. J. Zheng, Y. He, G. Wu, Q. J. Li, Y. J. Yan, Y. L. Xie, R. H. Liu, X. F. Wang and X. H. Chen*
 Hefei National Laboratory for Physical Science at Microscale and Department of Physics,
 University of Science and Technology of China, Hefei,
 Anhui 230026, People's Republic of China

The temperature dependence of electron spin resonance (ESR) was studied in $EuFe_{2-x}Co_xAs_2$ ($x = 0.0, 0.067, 0.1, 0.2, 0.25, 0.285, 0.35, 0.4$ and 0.5). The ESR spectrum of all the samples indicates that the g factor and peak-to-peak linewidth strongly depend on the temperature. Moreover, the peak-to-peak linewidth shows the Korringa behavior, indicating an exchange coupling between the conduction electrons and the Eu^{2+} ions. The linewidth, g factor and the integrate ESR intensity show anomalies at the temperature of the spin-density-wave (SDW). The linewidth below the SDW transition does not rely on the temperature. This gives the evidence of the gap opening at the T_{SDW} . The slope of the linewidth is closely associated to T_{SDW} and T_C . This exotic behavior may be related to the nesting of the Fermi surface.

PACS numbers: 31.30.Gs, 71.38.-k, 75.30.-m

The discovery of Fe-based high T_c superconductor provides a new family of materials to explore the mechanism of high- T_c superconductivity besides high- T_c cuprates superconductor¹⁻⁵. Ternary iron arsenides AFe_2As_2 ($A = Sr, Ca, Ba, Eu$) is one of parent compounds with $ThCr_2Si_2$ -type structure. In analogy with $LnFeAsO$ ($Ln = La-Gd$), AFe_2As_2 undergoes a structural phase transition and a spin-density-wave (SDW) transition, accompanied by the anomalies in electrical resistivity, magnetic susceptibility and specific heat. With doping electron or hole, the ground state of FeAs compounds evolves from SDW state to superconducting (SC) state.

$EuFe_2As_2$ is a unique member in the ternary iron arsenide family due to the large local moment of Eu^{2+} , which orders antiferromagnetically below 20K^{6,7}. Except for this AFM transition, the physical properties of $EuFe_2As_2$ are found to be quite similar with those of its isostructural compounds such as $BaFe_2As_2$ and $SrFe_2As_2$. Wu et al. have gave the evidence for a coupling between magnetism of Eu^{2+} ions and SDW ordering in FeAs layer⁷. Study on the interaction between the conduction electrons of FeAs layer and localized spins of Eu^{2+} layer gives significant information about the properties of FeAs layer. The ESR spectra in metals are very effective to study the interaction with the conduction electrons and local moments, which has been applied in high- T_c cuprates^{8,9}.

In this paper, we systematically studied the ESR spectra of the single crystals $EuFe_{2-x}Co_xAs_2$ ($x = 0, 0.067, 0.1, 0.2, 0.25, 0.285, 0.35, 0.4$ and 0.5). The g factor, peak-to-peak linewidth and the integrated ESR intensity all show anomalies at the T_{SDW} . The linewidth of all the samples shows the Korringa behavior above the T_{SDW} , indicating an exchange coupling between the conduction electrons and spin of the Eu^{2+} ions. The

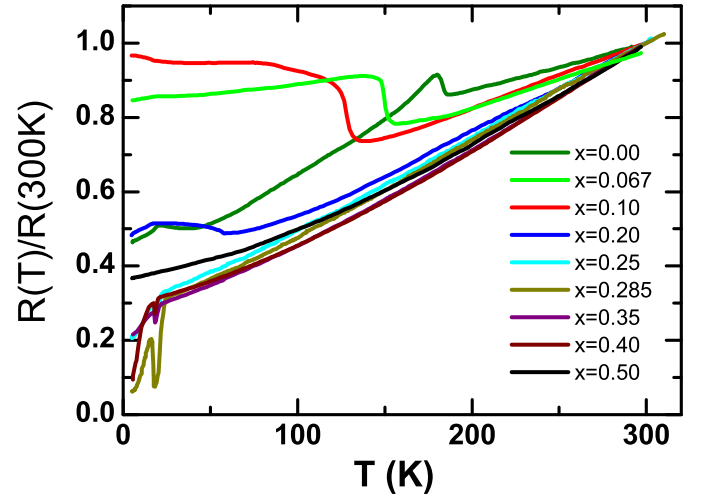


FIG. 1: (Color online) Temperature dependence of in-plane resistivity for the single crystals $EuFe_{2-x}Co_xAs_2$ with $x = 0, 0.067, 0.1, 0.2, 0.25, 0.285, 0.35, 0.4$ and 0.5 .

fact that linewidth becomes temperature independence below T_{SDW} gives the evidence of the gap opening at T_{SDW} . The slope of the linewidth shows interesting behavior with Co doping, and is closely related with the characteristic temperature: the T_{SDW} and the T_c .

High quality single crystals with nominal composition $EuFe_{2-x}Co_xAs_2$ ($x = 0, 0.067, 0.1, 0.2, 0.25, 0.285, 0.35, 0.4$ and 0.5) were grown by self-flux method as described for growth of $BaFe_2As_2$ single crystals with FeAs as flux¹⁰. Many shining plate-like $EuFe_{2-x}Co_xAs_2$ crystals were obtained. The ESR measurements of the single crystals were performed using a Bruker ER-200D-SRC spectrometer, operating at X-band frequencies (9.07 GHz) and between 110K and 300K. The resistance was measured by an AC resistance bridge (LR-700, Linear Research). It should be addressed that all results discussed as follows are well reproducible. We put the ab

*Corresponding author; Electronic address: chenxh@ustc.edu.cn

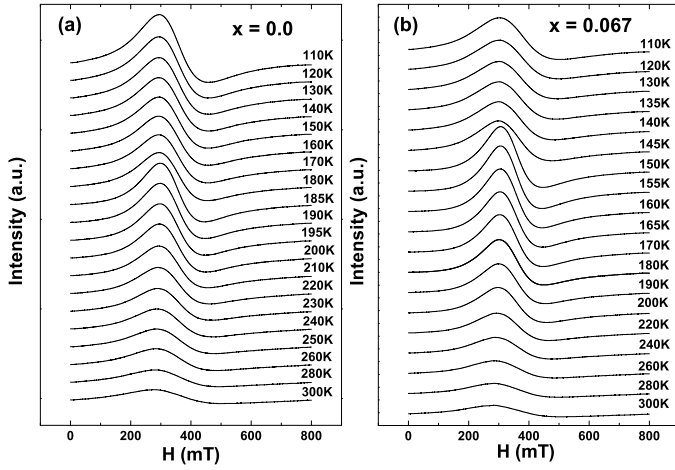


FIG. 2: Temperature dependence of ESR spectrum for (a): $x=0.0$ and (b): $x=0.067$.

plane of single crystals perpendicular to the magnetic field direction.

Fig.1 shows the temperature dependence of in-plane resistivity for single crystals $\text{EuFe}_{2-x}\text{Co}_x\text{As}_2$ with $x=0, 0.067, 0.1, 0.2, 0.25, 0.285, 0.35, 0.4$ and 0.5 . For parent compound EuFe_2As_2 , the resistivity shows a steep increase around 188 K, and reaches its maximum value around 180 K. It is associated with SDW and structure transition. The kink at about 20 K is related to antiferromagnetic ordering of Eu^{2+} moments. With Co doping, the SDW transition is gradually suppressed. For the crystal with $x=0.25$, the SDW transition was completely suppressed and shows superconducting transition at $T_c \sim 22$ K, but the resistance could not reach zero because of the antiferromagnetic ordering of the large local moment of Eu^{2+} ions. This issue is studied in separated work.¹¹ For the optimally doped crystal with $x=0.285$, the T_c reaches 24.5 K. For $x=0.35$ and $x=0.4$ samples, T_c decreases to 21 K and 20 K, respectively, while neither the SDW transition nor the superconductivity is observed for the heavily doped crystal with $x=0.5$.

Fig.2(a) and (b) show the temperature dependence of ESR spectra for the parent compound EuFe_2As_2 and one of the selected Co-doped samples $\text{EuFe}_{1.933}\text{Co}_{0.067}\text{As}_2$ in the temperature ranging from 110 K to 300 K, respectively. A well defined paramagnetic signal was observed in the whole temperature range. We ascribe the signal to the Eu ions because only weak signal can be detected in the BaFe_2As_2 single crystal. The intensity of the spectra is obviously suppressed with increasing temperature. The spectrum abruptly becomes narrow and the intensity is enhanced around T_{SDW} with increasing temperature. With further increasing temperature, the spectra broadens and the intensity decreases. The detailed analysis of the spectrum is discussed later on. In other Co-doped compounds, the similar signal has also been observed.

We analyzed the temperature dependence of ESR spec-

trum for $x=0.0$ and $x=0.067$ samples at the temperature ranging from 110 K to 300 K. For the two samples, the SDW transition temperatures are 188 K and 158 K determined from the resistivity as shown in Fig.1, respectively. Fig.3(a) illustrates the peak-to-peak linewidth (ΔH_{pp}) and the g factor as a function of temperature for the $x=0.0$ sample. ΔH_{pp} is defined as the width between the highest point and the lowest point in the temperature dependent ESR spectrum. The linewidth decreases linearly with decreasing temperature above the SDW transition temperature. This behavior is also observed in the isostructural EuCu_2Si_2 single crystals¹². ΔH_{pp} shows a sudden jump and begins to deviate from the linear trend at T_{SDW} . At the temperature below SDW transition, ΔH_{pp} becomes independent on temperature. The resonance field (H_c) to calculate the effective g factor is defined as the magnetic field corresponding to the midpoint between the highest and lowest points in the ESR spectrum. The effective g factor is calculated by the following formula: $g = \frac{h\nu}{\mu_B H_c}$. For the parent compound, the g factor monotonously increases with decreasing temperature, and a kink is observed at T_{SDW} . The ESR intensity of the parent compound obtained by numerical integration is illustrated in fig.3(b). It is found that the ESR intensity follows Curie-Weiss formula at high temperature with a kink at T_{SDW} . It is well known that ESR intensity is proportional to spin susceptibility, and the behavior of spin susceptibility is very much alike of DC susceptibility. This observation indicates that the same magnetic species contributes to the ESR spectrum as the dc susceptibility. It should be addressed that the drop of DC susceptibility at T_{SDW} cannot be observed because of the large magnetic moment of Eu^{2+} ,⁷ while the anomaly at T_{SDW} in spin susceptibility is very obvious as shown in Fig.3(b). Fig.3(c) and (d) show the temperature dependence of the linewidth, the g factor and the ESR intensity of the $x=0.067$ sample. The behavior of these three parameters is similar to that of the parent compounds, and an anomaly is observed at T_{SDW} . The ΔH_{pp} also shows the linear behavior above T_{SDW} . All these results confirm the interaction between the local moments of the Eu^{2+} and the conduction electrons in the FeAs layers. Comparing the $x=0.067$ sample with the parent compound, we find the jump of the linewidth at T_{SDW} is larger than the parent compound. Moreover, the drop of ESR intensity at the T_{SDW} for the $x=0.067$ sample is much sharper than the parent compounds.

The linewidth and the g factors of four typical Co doped crystals with $x=0.20, 0.25, 0.285$ and 0.40 are shown in Fig.4. As shown in Fig.1, the SDW transition temperature was suppressed down to 58 K for the $x=0.20$ crystal. The $x=0.25$ crystal with $T_c = 22$ K is in the underdoped region. The $x=0.285$ sample is at the optimal doping level and its $T_c=24.5$ K, nearly the same as the highest $T_c=25$ K in Co-doped BaFe_2As_2 .¹³ The $x=0.40$ sample with $T_c=20$ K is in the overdoped region. Strong temperature dependence of linewidth and the g factors are observed in all the samples. The linewidth

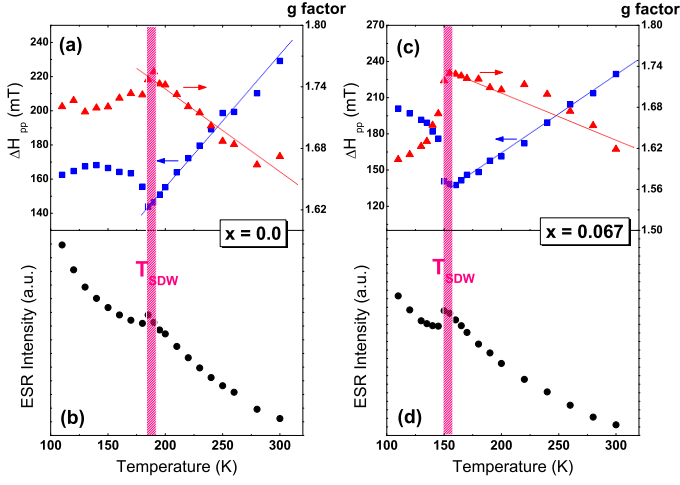


FIG. 3: (color online). Temperature dependence of g factor and ΔH_{pp} for the crystal with (a): $x = 0.0$ and (c): $x = 0.067$. Temperature dependence of ESR intensity for the crystal with (b): $x = 0.0$ and (d): $x = 0.067$. The blue line shows the fitting with linear behavior.

of all the samples follows the linear temperature dependence. This phenomenon is consistent with the behavior observed in the $x=0$ and 0.067 samples above T_{SDW} as shown in Fig.3(a) and (c). The g factor of all the four samples increases monotonously with decreasing temperature. No anomalies are found in these four compounds.

In order to systematically investigate the effect of Co doping in $EuFe_{2-x}Co_xAs_2$, the ESR spectrum of the other samples with different doping level was measured. It is found that the temperature dependence of linewidth for all the samples shows the same behavior. The linear temperature dependent linewidth is observed in all the samples above T_{SDW} . Figure 5 illustrates the slope of the linewidth, T_{SDW} and T_c as a function of Co doping. It is striking that the slope of the linewidth shows a close relation with the characteristic temperature T_{SDW} and T_c . As shown in Fig.5, the SDW ordering is gradually suppressed and T_{SDW} decreases with increasing Co doping. It is intriguing that the slope of the linewidth shows the same behavior as that of T_{SDW} , and the slope of the linewidth decreases with increasing Co doping in the underdoped region. With further increasing the Co doping, the superconductivity emerges and the slope of linewidth begins to increase. In the superconducting region, the slope of linewidth shows the same behavior as T_c . Both the slope of linewidth and T_c exhibit a dome-like behavior with increasing the Co doping. The evolution of the slope of linewidth with Co-doping is qualitatively consistent with that of T_{SDW} and T_c . Spin relaxation of magnetic moments in conventional metals mainly depends on the relaxation times between local moments and itinerated electrons, and spin-lattice relaxation time for itinerated electrons and spin-lattice relaxation time for local moments^{14–16}. The linewidth is a measurement of the relaxation for the spin system. The exchange in-

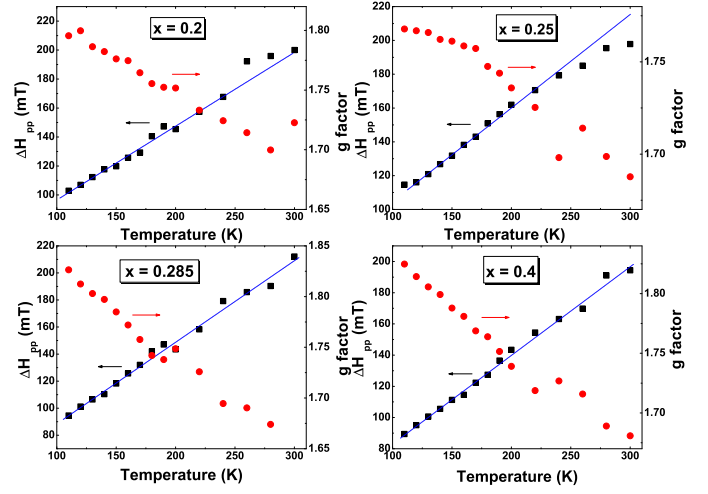


FIG. 4: (color online). Temperature dependence of g factor and ΔH_{pp} for the crystal with (a): $x=0.20$; (b): $x=0.25$; (c): $x=0.285$ and (d): $x=0.4$. The blue line shows a linear fitting.

teraction between local moments and conduction electrons results in a temperature-linear contribution to the total ESR linewidth⁸. It follows the Korringa behavior $\Delta H = \Delta H_K + \Delta H_{res}$. ΔH_{res} is the residual linewidth and ΔH_K is the Korringa broadening given by $\Delta H_K = \frac{\pi K_B T}{g \mu_B} (J_{Ss} \rho(\epsilon_F))^2$. Here μ_B is the Bohr magneton, K_B is the Boltzmann constant, J_{Ss} is the exchange interaction between the local moments (S) and the spin of the conduction carriers (s), $\rho(\epsilon_F)$ is the density of states at Fermi surface. The local moment should come mainly from the Eu atom in $EuFe_{2-x}Co_xAs_2$ system. The linear linewidth above T_{SDW} for all the samples follows the Korringa law. When SDW transition happens, the linear linewidth behavior is destroyed. The 'free-ion' g factor for Eu is normally given as 1.993 in an insulating host¹⁵. The g factor of Eu ions in these materials is much smaller than 1.993 in the whole temperature range. The shift of g factor is very sensitive to the temperature, and a kink shows up at the temperature corresponding to SDW transition. This behavior is different with the LaOFeAs system in which ferromagnetic fluctuation from local moment of Fe ions was observed¹⁶. Such difference could be related to the large local moments of Eu^{2+} . The ESR integral intensity, which is proportional to the spin susceptibility, also shows anomalies at T_{SDW} . In the parent compounds the linewidth becomes independent on the temperature below T_{SDW} , so the linewidth slope is zero. If it is assumed that the Korringa law is applicable below T_{SDW} , then the $\rho(\epsilon_F)$ must be zero. This result means that the density of state losses at the Fermi surface and a gap opens at the temperature below T_{SDW} . Such behavior of linewidth has been observed in the Kondo insulator CeNiSn¹⁷. The slope of linewidth exhibits an interesting behavior with the Co doping, and it shows a close relation with the characteristic temperature T_{SDW} and T_c . Because the J_{Ss} between the Eu^{2+} and the conduction

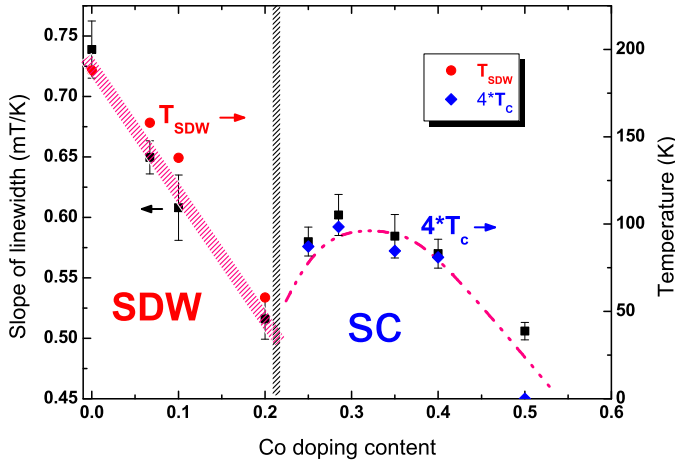


FIG. 5: (color online). The slope of peak-to-peak linewidth as a function of the Co doping content. The black squares denote the slope of linewidth, and the red circles present the SDW transition temperature and the blue diamonds presents the $4T_c$.

electrons does not change with Co doping, the difference of the slope must come from the density of state at Fermi surface. Recently, Terashima et al.¹⁸ observed isotropic SC gaps which depend on the nesting conditions of Fermi surface in the iron-based superconductors. The superconductivity in this system is related to the Fermi surface topology¹⁹. The Fermi surface nesting maybe play an important part in the superconductivity, and the nesting of Fermi surface has a strong effect on the slope of the linewidth. There are two possible explanation for the

SDW ordering. One explanation is that the Fermi surface is perfectly nesting for the parent compounds, resulting in SDW ordering. With Co doping, the Fermi surface nesting is gradually destroyed, so that the slope decreases with the Co doping in the SDW region. While in the SC region, the Fermi surface nesting condition is changed, and the superconductivity is closely related to the Fermi surface nesting based on the study by Terashima et al.¹⁸. The behavior of the slope associated with the T_{SDW} and T_c could be related to the complicated nesting of Fermi surface.

In conclusion, we studied the temperature dependence of ESR spectrum for single crystals $EuFe_{2-x}Co_xAs_2$ ($x=0, 0.067, 0.1, 0.2, 0.25, 0.285, 0.35, 0.4$ and 0.5). Strong temperature dependence of the g factor and ΔH_{pp} are observed in all the samples. The linewidth, the g factor and the ESR intensity all show anomalies at the SDW temperature. The linewidth for all the samples above T_{SDW} shows the Korringa behavior. These results indicate the exchange interaction between the local moments of Eu^{2+} and the conduction electrons in FeAs layers. A gap opening at the SDW transition is evidenced by the fact that the linewidth does not change below the SDW temperature. The slope of the linewidth is strongly dependent on the Co doping content, and is closely associated with T_{SDW} and T_c . Such behavior maybe related to the complicated Fermi surface nesting.

This work is supported by the Nature Science Foundation of China and by the Ministry of Science and Technology of China (973 project No: 2006CB601001) and by National Basic Research Program of China (2006CB922005).

- ¹ Y. Kamihara, T. Watanabe, M. Hirano, and H. Hosono, *J. Am. Chem. Soc.* **130**, 3296(2008).
- ² X. H. Chen and T. Wu, G. Wu, R. H. Liu, H. Chen and D. F. Fang, *Nature* **453**, 761(2008).
- ³ G. F. Chen, Z. Li, D. Wu, G. Li, W. Z. Hu, J. Dong, P. Zheng, J. L. Luo, and N. L. Wang, *Phys. Rev. Lett.* **100**, 247002(2008).
- ⁴ Z. A. Ren, G. C. Che, X. L. Dong, J. Yang, W. Lu, W. Yi, X. L. Shen, Z. C. Li, L. L. Sun, F. Zhou and Z. X. Zhao, *Europhys. Lett.* **83**, 17002(2008).
- ⁵ M. Rotter, M. Tegel, D. Johrendt, *Phys. Rev. Lett.* **101**, 107006(2008).
- ⁶ Zhi Ren, Zengwei Zhu, Shuai Jiang, Xiangfan Xu, Qian Tao, Cao Wang, Chunmu Feng, Guanghan Cao and Zhuan Xu, *Phys. Rev. B* **78**, 052501 (2008).
- ⁷ T. Wu, G. Wu, H. Chen, Y. L. Xie, R. H. Liu, X. F. Wang and X. H. Chen, arXiv:0808.2247. *J. Mag. Mat.* (in press).
- ⁸ D. Shaltiel, C. Noble, J. Pilbrow, D. Hutton, E. Walker, *Phys. Rev. B* **53**, 12430 (1996).
- ⁹ V. Kataev, Yu. Greznev, G. Teitel'baum, M. Breuer and N. Knauf, *Phys. Rev. B* **48**, 13042 (1993).
- ¹⁰ X. F. Wang, T. Wu, G. Wu, H. Chen, Y. L. Xie, J. J. Ying, Y. J. Yan, R. H. Liu, X. H. Chen, *Phys. Rev. Lett.* **102**, 117005(2009).
- ¹¹ Q. J. Zheng, Y. He, T. Wu, G. Wu, H. Chen, J. J. Ying, R. H. Liu, X. F. Wang, Y. L. Xie, Y. J. Yan, Q. J. Li and X. H. Chen, unpublished.
- ¹² C. D. Cao, R. Klingeler, N. Leps, H. Vinzelberg, V. Kataev, F. Muranyi, N. Tristan, A. Teresiak, Shengqiang Zhou, W. Löser, G. Behr and B. Büchner, *Phys. Rev. B* **78**, 064409 (2008).
- ¹³ X. F. Wang, T. Wu, G. Wu, R. H. Liu, H. Chen, Y. L. Xie, X. H. Chen, *New J. Phys.* **11**, 045003 (2009).
- ¹⁴ R. H. Taylor, *Advances in Physics* **24**, 681-791 (1975).
- ¹⁵ S. E. Barnes, *Advances in Physics* **30**, 801-938 (1981).
- ¹⁶ T. Wu, J. J. Ying, G. Wu, R. H. Liu, Y. He, H. Chen, X. F. Wang, Y. L. Xie, Y. J. Yan, and X. H. Chen, *Phys. Rev. B* **79**, 115121 (2009).
- ¹⁷ S. Mair, H.-A. Krug von Nidda, M. Lohmann and A. Loidl, *Phys. Rev. B* **60**, 16409 (1999).
- ¹⁸ K. Terashima, Y. Sekiba, J. H. Bowen, K. Nakayama, T. Kawahara, T. Sato, P. Richard, Y.-M. Xu, L. J. Li, G. H. Cao, Z.-A. Xu, H. Ding, T. Takahashi, *Proceedings of the National Academy of Sciences of the USA (PNAS)* **106**, 7330-7333 (2009).
- ¹⁹ Y. Sekiba, T. Sato, K. Nakayama, K. Terashima, P. Richard, J. H. Bowen, H. Ding, Y.-M. Xu, L. J. Li, G.

H. Cao, Z.-A. Xu, T. Takahashi, New J. Phys **11**, 025020 (2009).